A method for controlled target strength measurements of pelagic fish, with application to European anchovy (*Engraulis encrasicolus*)

Doray Mathieu [1, *], Berger Laurent [2], Le Bouffant Naig [2], Coail Jean-Yves [3], Vacherot Jean-Philippe [4], De La Bernardie Xavier [5], Morinière Pierre [6], Lys Elisabeth [5], Schwab Romain [2], Petitgas Pierre [1]

[1] Unité Écologie et Modèles pour l'Halieutique, Ifremer Nantes, Rue de l'Ile d'Yeu, BP 21105, 44300 Nantes Cedex 3, France
[2] Service Acoustique Sous-marine et Traitement de l'Information, Ifremer Brest, Brest, France
[3] Service Ingénierie et Instrumentation Marine, Ifremer Brest, Brest, France
[4] Laboratoire de Technologie et de Biologie Halieutique, Ifremer Lorient, Lorient, France
[5] UMR SUBATECH, CNRS (IN2P3) - École des Mines de Nantes - Université de Nantes, Nantes, France
[6] Aquarium La Rochelle, La Rochelle, France

* Corresponding author : Mathieu Doray, tel: + 33 (0)2 40 37 41 65; fax: + 33 (0)2 40 37 40 75 ; email address : mathieu.doray@ifremer.fr.

Abstract :

Measuring fish target strength (TS) in the wild is challenging because: (i) TS varies versus physical (orientation relative to the incident sound wave, size, and depth) and physiological fish attributes (maturity and condition), (ii) the target species and its aforementioned attributes are difficult to assess in near real time, and (iii) in the case of packed fish schools, accepted echoes may originate from multiple unresolved targets. We propose a method for controlled TS measurements of densely packed small pelagic fish during daytime, based on the joint use of a Remotely Operated Towed Vehicle, "EROC", with a pelagic trawl fitted with a codend opening system, "ENROL". EROC, equipped with a 70-kHz split-beam echosounder (Simrad EK60) and a low-light black and white camera, can be moved inside the fishing trawl. Pelagic fish are funnelled into the open trawl and their TS is measured in the middle of the net, where small groups actively swim towards the trawl mouth. The swimming behaviour allows for near-dorsal TS to be measured, minimizing the large effect of incidence angle on TS variability. The EROC camera, located near the open codend, provides optical identification of the species. This method was used to measure the TS of European Anchovy, *Engraulis encrasicolus* in the Bay of Biscay during 2014. The mean, near dorsal TS was −43.3 dB, for a mean fork length of 12.5 cm. This value is compared to published values of clupeiforms mean TS obtained for a range of natural incidence angles and discussed in the light of TS modelling results obtained for E. encrasicolus.

Keywords : acoustics, deformed cylinder model, Engraulis encrasicolus, remotely operated vehicle, target strength, video

Introduction

Knowledge of target strength (TS) of single fish is important for acoustic target classification (Barange, 1994; Doray *et al.*, 2006), and abundance estimation (Rose, 1992; Jech and Horne, 2001). However, measuring fish TS in the wild is challenging because: i) TS largely varies versus physical (orientation relative to the incident sound wave, size, and depth) and physiological fish attributes (Horne, 2000), ii) the target species and its aforementioned attributes are difficult to assess at the same time as acoustic measurements (Simmonds and MacLennan, 2005), and iii) multiple targets echoes can be accepted as single target ones in the case densely packed fish schools (Soule *et al.*, 1995). Acoustic-Optic Systems (AOS) combining scientific echosounders and camera have been successfully used to record TS of loosely aggregated fish, while observing species (Doray *et al.*, 2007; Ryan *et al.*, 2009; O'Driscoll *et al.*, 2013), and, using a stereo camera, observing species, size, and orientation (Kubilius and Ona, 2012).

During daytime, small pelagic fish congregate in schools that are too densely packed to resolve individual targets with hull-mounted echosounders (Sawada *et al.*, 2009). At night, small pelagic fish schools often disperse and migrate near to the surface (Fréon and Misund, 1999) where they cannot be detected by down-projecting hull-mounted echosounders. Moreover, at night, small pelagic fish usually mix with other scatterers. Despite these potential complications, TS measurements have been made at night using hull-mounted echosounders (Foote, 1987; Barange *et al.*, 1996; Peltonen and Balk, 2005; Zhao *et al.*, 2008), but in these cases, the fish in the study areas were dominated by the target species.

In these studies, the distribution of fish orientation relative to the incident sound wave is assumed to represent the average incident angle for all measures of the population (Simmonds and MacLennan, 2005). This assumption might not be valid if the fish exhibit diel swimming behaviour. To mitigate this potential problem, others have lowered transducers and a camera closer to the fish targets to: i) better resolve individuals and ii) simultaneously assess the species and their orientations (Ona, 2003; Sawada et al., 2009).

The lack of TS values for European anchovy (*E. encrasicolus*) and sardine (*S. Pilchardus*) in the literature has been pointed out by the Working Group on Acoustic and Egg Surveys for Sardine and Anchovy in the Bay of Biscay and Iberican peninsula areas (ICES, 2008). In the Bay of Biscay, dense sound scattering layers (SSL) are observed near the surface at night in springtime. In this case, the TS of small pelagic fish cannot be distinguished from that of other scatterers. Therefore, TS measurements must be made during daytime,

within highly packed small pelagic fish schools. We present a method to measure daytime TS of small pelagic fish in their natural environment, while observing the species, its length, and orientation relative to the incident acoustic wave (incident angle). The method involves the use of a pelagic trawl fitted with a codend opening system, 'ENROL', to herd and orient fish, and Ifremer's Remotely Operated Towed Vehicle (ROTV), 'EROC', to make acoustic measurements and video observations. The method was used to assess the daytime TS of European anchovy (*Engraulis encrasicolus*) in the Bay of Biscay. Reults are compared to published values of clupeiforms mean TS obtained for a range of natural incidence angles and discussed in the light of TS modelling results obtained for *E. encrasicolus*.

Materials and Methods

The ROTV EROC (Engin Remorqué d'Observation de Chalut) (Figure 1a) was originally used by the Ifremer Research and Technological Development Department for trawl observations. The 2.3-m long, 1.6-m wide and 1.6-m high ROTV weighs 400 kg and is equipped with a stainless steel frame, anodised aluminium rotors, and high density foam floats ensuring positive buoyancy. It is towed behind the vessel at the end of a 21-mm diameter, 1000m long cable fitted with optic fibre. It can be moved, in real time, in the vertical and horizontal planes using two Magnus effect rotors. Its positive buoyancy housing allows for deployments as deep as 300 m, at speeds from 2 to 4 knots, nominally 3 knots. It is enclosed in a protective cage that ensures safe deployment and retrieval through the stern trawler ramp. The ROTV EROC is equipped with motion and pressure sensors recording roll, pitch and depth values every 2 seconds, and a black and white, high definition, low-light pan and tilt camera, whose images are displayed in real time for the pilot to locate and manoeuvre the ROTV. The camera outputs can be recorded in real time by a DVD recorder. A split-beam echosounder (Simrad EK60) fitted with a deep water 70-kHz transducer (Transonics) with a nominal 7° beam angle was added to the system. To assess the effect of pressure and temperature variations on the transducer, on-axis calibrations of the echosounder were performed at 10, 30, 55 and 70 m depth using a standard method (Foote *et al.*, 1987), on May 30, 2015.

The echosounder was operated at the highest transmit rate (20 transmissions per second, on average) and shortest pulse duration (128 μs) available, to provide 30-cm horizontal and 10-cm vertical sampling

resolutions.

The codend of the pelagic trawl (2 doors, headline = 57 m, foot rope = 52 m) was replaced with a cylindrical frame of neutral buoyancy called the "ENROL" (Engin Remorqué d'Observation non Léthale, Figure 1b), to allow fish escapement (Figure 2). The objective was to funnel the fish through the open trawl, break up the schools, and allow TS to be measured from dispersed fish swimming in the same direction inside the trawl. As TS were recorded for several hours, the ENROL was configured to allow fish to escape the trawl, to reduce fish mortality during the experiments.

The method can be summarized as follows: i) during daytime, detect schools of pelagic fish using the vessel's hull-mounted echosounders; confirm the schools are monospecific and identify the species using a midwater trawl; and shoot the ENROL-equipped trawl in the area; ii) deploy EROC; iii) locate the trawl using the EROC echosounder, while keeping the ROTV at 10-m depth, to avoid entanglement in the net; iv) position the EROC 2 m above the central part of the trawl using the camera; v) record TS of fish attempting to escape the trawl by actively swimming toward the mouth; and vi) bring EROC closer to the ENROL every hour to observe and identify fish inside the trawl.

The EROC-ENROL method was developed during the PELGAS surveys (Doray *et al.*, 2014) in 2011, 2012, 2014 and 2015. The TS measurements presented in this paper were made on May 31, 2014 and June 01, 2014, between 10:00 and 18:00 GMT (local time = GMT +2), onboard Ifremer's R/V Thalassa during the PELGAS2014 survey. The system was deployed (N=4 trawl hauls) in an area of the Bay of Biscay (mean depth of 64 m) (Figure 2), populated by dense fish school aggregations mostly (mean proportion = 88%) comprised of European Anchovy (mean total length L=12.5-cm; SD=0.8 cm, Figure 3).

Acoustic data were processed (Movies3D software; Trenkel et al., 2009) and archived in the international hydroacoustic data format (HAC; ICES, 2005) with a −80 dB threshold. All single-target echoes with a TS greater or equal to −60 dB were first selected using the EK60 SIMRAD algorithms (Andersen, 2005), implemented with the parameters presented in Table 1. As the number of single echoes selected using this algorithm was low, in comparison to the large number of single targets visible on the echograms, we applied an alternative single-echo detection algorithm (Soule et al., 1997), reviewed in ICES (1999), with ad-hoc parameters presented in Table 1 to extract more single echoes. As single echoes were detected in reflections

from the trawl head and footropes, as well as from fish, all non-fish TS measurements were removed via visual scrutiny of the TS echogram. The Movies3D target tracking algorithm was applied to the single-fish echoes selected by both algorithms, to derive information on fish swimming behaviour. Refer to appendix 1 for detailed descriptions of the Soule et al. (1997) single-echo detection and tracking algorithm implementations in Movies3D. Acceptable tracks had at least 10 detections, no more than one missed observation between consecutive detections, and a maximum speed of 5 knots (2.57 m s^{-1}). This speed threshold is less than the theoretical maximum burst speed of 6.25 knots (i.e. 25 body length.s^{-1}) of a 12.5 cm fish (Wardle, 1975).

The EROC depth was adjusted during the TS recordings, to follow variations in the trawl depth. According to the EROC pressure sensor recordings, the ROTV-depth variations were negligible at the temporal scale of a track (EROC average depth variation during TS recordings: 2cm, SD=1cm). The target depth variations during a track were therefore computed based on their positions in the acoustic beam, without correcting for EROC depth variations. The EROC pitch and roll angles were recorded once every 2 seconds, which is too low compared to the echosounder transmit rate (20 transmissions s^{-1} on average) and the track duration (mean track duration = 1 s) to allow to compute single targets incidence angles by correcting their positions for EROC pitch variations within each transmission or track. In an attempt to assess the uncertainty introduced by the EROC motion in the target orientation estimates, EROC pitch and roll averages and SD were computed over all tracks (Table 2). These values being low (EROC average roll during all tracks: 4.1°, SD = 1.4°; EROC average pitch during all tracks: 3°, SD = 3°)), fish single targets orientations were not corrected for EROC pitch and roll variations.

The mean target heading of each track, $h_{track,}$ was computed as the average of the i measurements of heading, h_i in the horizontal plane between consecutive target positions in the acoustic beam: $h_i= atan (dy_i/dx_i)$, where dx_i is the target displacement to the north, and dy_i is the target displacement to the east (heading north = 0°, anti-clockwise angles). The difference between h_{track} and the vessel heading during the track was used as a proxy for fish heading in the net.

A mean target pitch angle during the track, p_{track}, was computed as the average of the i measurements of pitch p_i in the vertical plane between successive target positions in the acoustic beam: $pitch_i = atan ($

135    $\dfrac{dz_i}{\sqrt{dx_i{}^2 + dy_i{}^2}}$), where dx_i is the target displacement to the north, dy_i is the target displacement to the east and dz_i is the target depth variation (horizontal pitch angle = 0°, positive values downward).

Results

Calibrations results showed a good agreement between the data and the beam model at all depths (mean Root Mean Square, RMS = 0.2 dB, standard deviation, SD = 0.02 dB, see Table 3 in supplementary material).

140 Significant negative linear relationships were found between the depth covariate and transducer gain, and alongships and athwartships beam angles (see Table 3 and Figure 11 in supplementary material). No significant relationship was found between the depth covariate and S_a correction. The difference in gain (transducer gain plus S_a correction) between 10 and 70 m was 0.9 dB. This depth-related echosounder gain variation would induce a 1.8 dB difference between TS measurements performed at 10 versus 70 m depth.

145 No relationship was found between the echosounder calibration parameters and the temperature-at-depth.

A total of four acoustic datasets, recorded on May 31, 2014 and June 01, 2014 were selected after single echo detection, tracking, and TS-echogram inspection (Table 2, Figure 5). As fish TS were recorded between 55- to 60-m depth, the calibration gains obtained at 55 m depth were applied to all targets. Relative to Simrad's single-echo detection algorithm, our implementation of the algorithm proposed by Soule et al.

150 (1997), denoted below as Movies3D', detected 60% more fish single targets (1287 / 495), 71% more tracks (76 versus 28), and 160% more tracks per dataset (322, SD=122 versus 124, SD=40). The tracks derived from both algorithms were of similar length (17, SD=2 versus 18, SD=4) (Table 2, Figure 5).

Fish single targets σ_{bs} ($TS=10*log10(\sigma_{bs})$; Simmonds and MacLennan, 2005) were averaged over tracks to filter out the intra-track variability (e.g. incidence angle variations due to fish position in the beam, tilt

155 angle and tail beat effect), then converted to logarithmic TS. The mean TS per track distribution obtained using the Movies3D algorithm over all datasets was nearly symmetrical, centred around the mean = -43.3 dB, with 5% and 95% quantiles equal to -46.3 and -41.5 dB, respectively (Figure 6). The mean TS per track distribution obtained using the Simrad single echo detection algorithm over all datasets was skewed toward low values, with a mean of -43.7 dB and a larger spread (5 and 95% equal to -47.2 and -41.7 dB ,

160 respectively (Figure 6). The TS distributions of non-tracked single echoes displayed higher spread, as well as

secondary modes (Figure 6). As the Movies3D method provided a higher number of tracked single targets, and therefore more potential information on the fish swimming behaviour in the trawl, as well as a mean TS per track distribution similar to those obtained with the Simrad algorithm, we retained the results derived from the single echoes detected with the Movies3D method for further analysis.

165   The fish targets global pitch angles during tracks p_{track} were unimodal in all datasets, centered around a mean value = -0.6° (SD = 0.8°) (Figure 7). We then assumed that, apart from EROC pitch and roll, the fish were swimming almost horizontally in the trawl.

      Substituting the mean TS and fish total length measurements (L) from this study in the log-linear TS versus L(in cm) relationship: $TS = 20*log_{10}(L)+b_{20}$, the b_{20} value is -65.2 dB.

170   The fish headings in the horizontal plane during tracks relative to EROC heading (p_{track}-heading$_{EROC}$) were unimodal in all datasets, centred around a mean value = -3.9°, and narrowly spread to the right tail (SD = 7.7°) (Figure 8). This indicates that most of the fish were swimming almost parallel to the trawl. Video recording confirmed these results and further demonstrated that the fish were swimming towards the trawl mouth, and were progressively swept by the current toward the open codend. No relationship was found

175 between the mean TS per track and the track parameters (no. of pings, angles, and depth variation) at the scale of the datasets.

      All fish species tended to swim upcurrent, toward the mouth of the trawl, even after having escaped the trawl through the open codend. Most fish swam upcurrent until exhaustion, some escaped through the mesh. When fish reached exhaustion, they were washed out throughout the codend. Small pelagic fish showed very

180 strong school fidelity, sometimes swimming outside the trawl alongside with their conspecifics inside the trawl. All small pelagic fish species inside and outside the trawl showed a strong attraction to light, leading sometimes to escapement, when the EROC lights were switched on at close range.

Discussion and Conclusion

The EROC ROTV was first deployed alone during daytime at low speed (3.8 knots), in an area with high

185 density of pure anchovy schools, in an attempt to measure anchovy TS inside schools. No fish TS were recorded in the schools in that way, as fish were too densely packed to allow for single fish TS detection. The ENROL open trawl allowed to small pelagic fish to herd and scatter inside the net where they could be

individually insonified by the EROC echosounder, hence enabling the recording of small pelagic fish TS during daytime. We observed that the school cohesion was disrupted by the strong current inside the trawl, whereas small pelagic fish quickly reformed schools after exiting the trawl through the ENROL device. This suggest that recording TS inside the trawl with the EROC increases the odds of detecting single echoes of schooling small pelagic fish, compared to measurements conducted on densely packed schools entering the trawl with e.g. the AOS system (Ryan et al., 2009).

Unsuccessful attempts were made to record the TS of a calibration sphere inside the trawl, to assess the effect of the trawl mesh on TS measurements. We assumed that the effect of the trawl mesh on acoustic measurements was negligible.

The Movies3D implementation of the Soule et al. (1997)'s algorithm and Simrad's algorithm are based on the same single target selection principles, but differ in their parameterisation. The proposed parameterisation allows for the selection of more candidate single targets than Simrad's. The potential multiple targets detected inside the anchovy groups by the Movies3D parameterisation of Soule et al. (1997)'s algorithm were filtered out during the target tracking step, yielding a higher number of tracked fish single targets than Simrad's algorithm (Figure 5, Table 2). The use of the proposed single target detection method included more datasets in the analysis that would not have been considered if analysed using the Simrad's algorithm, because of single echoes detection shortage. The higher number of tracked single targets obtained with the Movies3D method also provided: i) a more symmetrical, unimodal, and narrow distribution of mean TS per track, resulting in a more accurate and precise average TS for anchovy; ii) more tracks, providing more information on the fish swimming behaviour in the trawl.

Attempts were made to record TS of fish exiting the ENROL at the end of the trawl. These were commonly about 20 dB lower than the fish TS recorded inside the trawl. Video observations conducted by the EROC near the ENROL, as well as fish depth variations derived from TS tracking suggest that fish exiting the trawl were heavily tilted (~60°), which likely explains their lower TS values. These low TS values were not retained, as they were not thought to reflect the average, typical, fish swimming behaviour, and could not be distinguished from single targets of other weak scatterers detected around the trawl.

The fish single target positions were not corrected for EROC pitch and roll. As the targets pitch

8

215 distribution during tracks suggests that fish were on average swimming almost horizontally, we instead used

the small (less than 10°, cf. Table 2) EROC pitch and roll variations to further explore the fish acoustic

directivity pattern.

This study presents TS values of 12.5 cm *E. encrasicolus* swimming almost horizontally. The mean TS

value is 6 dB higher than the theoretical TS predicted for a 12.5 cm *E. encrasicolus* using either the Foote

220 (1987) TS(L) equation for physostomous fish, or the equations used by the French, Spanish and Portuguese

research institutes to assess European Anchovy populations biomass (ICES, 2008). Our TS estimate is 2.1 dB

higher than those predicted by the Ona (2003) TS(L, depth) equation for a herring swimming at 60-m depth.

However, these equations resulted from averages of fish TS measured for a larger range of incidence angles

than in our study. TS for fish with a swimbladder is maximum when the maximum swimbladder dimension is

225 perpendicular to the acoustic beam axis, i.e. when the fish swim almost horizontally (Simmonds and

MacLennan, 2005). In this paper, the anchovy measured using the EROC-ENROL method were swimming

almost horizontally, with a low tilt angle SD, which is not representative of their natural behaviour. The mean

TS value presented in this paper was hence computed in a narrow area of the fish directivity pattern, near its

maximum. This likely explains why the *E. encrasicolus* TS value derived using the EROC-ENROL method

230 is largely higher than the theoretical values predicted using models established over a wider fish tilt angle

distribution.

In a attempt to corroborate our TS measurements, a model of acoustic scattering by *E. encrasicolus* was

developed to investigate the effect of incidence angle and swimbladder compression on fish TS. The

swimbladder accounting for 90% or more of the fish acoustic scattering (Foote, 1980), the other organs

235 contribution to total backscatter was neglected. 3-dimensional (3D) representations of the swimbladders were

derived from 3D computed X-ray tomographic (CT) imaging. *E. encrasicolus* specimen were collected in the

Bay of Biscay and stocked in a 1.5 m deep tank at Aquarium La Rochelle for 7 months. A total of 33 fish

were anaesthetised using eugenol for 10-15 minutes and immediately frozen in liquid nitrogen, to avoid post-

mortem gas release from the swimbladder. Five suitable specimen (mean total length = 10.5 cm, SD = 0.5

240 cm) were selected after X-ray examination to ensure that the swimbladders were intact and inflated. The five

E. encrasicolus were examined frozen with Subatech's RX Solutions EasyTom XL 150 X-ray CT scanner.

9

The high image contrast between the gas-filled swimbladder and surrounding organs enabled the precise assessment of the swimbladder boundaries from the CT images (Figure 9). 3D representations of the swimbladders and surrounding tissues were built with the MeVisLab software, using the thresholding method (Figure 9). Key positional and morphological features were derived from swimbladders 3D representations of each anchovy. Swimbladder descriptors means and SD (Table 3) were used to parameterise a modal series based deformed cylinder acoustic scattering model (Stanton, 1988, 1989), offset by the average swimbladder tilt angle in the fish (4.2°, SD = 0.9°). The model was applied to virtual anchovies randomly distributed in the equivalent aperture of the measured anchovies targets (11°), to derive TS distributions for several frequency:fish tilt angle:swimbladder aspect ratios combinations. TS were predicted for each virtual anchovy as a function of total length, scaled to the observed anchovies length (L~ N (12.5 , 0.5)), frequency (38 and 70 kHz) and over tilt angles taken in 4 normal distributions of identical mean and increasing SD: N (-0.5°,1), N (-0.5°,5), N(-0.5°,10) and N(-0.5°,15). The later tilt angle distribution corresponds to various "natural" tilt angle distributions previously measured and used for pelagic species (McClatchie et al., 1996; Faessler *et al.*, 2013). Changes of swimbladder morphology with pressure were simulated by using three different mean aspect ratio: 10 (fully inflated), 15 (partially deflated), and 20 (deflated). TS were predicted for 100 virtual anchovy for each frequency:fish tilt angle:swimbladder aspect ratio combination. The fish length ratio, swimbladder tilt angle and swimbladder curvature values were randomly taken from normal distributions with means and standard deviations equal to those of the average 3D swimbladder representation (Table 3).

The TS distributions obtained at the 38 and 70 kHz frequencies with the three swimbladder aspect ratios and four pitch angle distributions are presented in Figure 10. Modelled mean TS values (computed in the linear domain and converted into logarithmic TS) are very close at the 38 and 70 kHz frequencies for fish tilt angle distribution SDs equal to 1 and 5°, and rapidly diverge when the fish tilt angle variance increases. Modelled and observed TS distributions show similar shape, mean and spread at the 70 kHz frequency in the case of virtual fish swimming almost horizontally (fish tilt angle distribution ~ N (-0.5 , 1)), with swimbladder aspect ratios ranging from 15 to 20 (i.e. for swimbladder compression factors ranging from 1.5 to 2). This compression factor range is less than expected for a free-balloon model, according to Boyle's law (2.6 at 60 m depth). Zhao et al (2008)'s TS measurements of Japanese Anchovy (*Engraulis japonicus*)

270   suggest that the TS depth-dependence of this species might follow Boyle's law. Their study was however based on a relatively small sample, collected within a narrow (20-40 m) and more shallow depth layer than in our study, and without information on fish tilt angles. On the other hand, Ona (2003)'s empirical TS(L,depth) equation based on extensive TS measurements at depths down to 500 m predicts a compression factor (1.56) within the range of our modelling results, for a 12.5 cm herring (*Clupea harengus*) swimming at 60-m depth.

275   Moreover, our modelling results show that an increase of the fish tilt angle distribution SD from 1° (near horizontal swimming behaviour) to 15° ("natural" swimming pattern) leads to a 2 to 3 dB decrease of the mean TS values, at the 38 and 70 kHz frequencies, respectively. Updating the log-linear TS versus length relationship for *E. encrasicolus* with the 2dB decrease predicted at 38kHz yields a b_{20} values of -63.2 dB. This value is in line with the TS predicted at the 38 kHz frequency by the Ona (2003) TS(L, depth) equation

280   for a 12.5 cm herring swimming at 60-m depth. Assuming that the *E. encrasicolus* swimbladder compression factor at 60 m depth lies in the wild between 1.5 and 2, which seems likely according to Ona (2003)'s study on herring, our modelling results confirm that the measured TS value presented in this paper is a realistic estimate of the maximum TS of a 12.5 cm *E. encrasicolus* at 60-m depth, that could be used to scale and evaluate future TS models for this species.

285   Complementary modelling and *ex-situ* experiments should be conducted to derive robust TS(L, depth) equations that account for the natural tilt angle distribution of *E. encrasicolus*. The use of a pan and tilt transducer on the EROC would facilitate sampling of TS over a large range of incidence angles and at different depths.

        In summary, the EROC/ENROL method can be used to measure TS of small pelagic fish while

290   controlling for species, length, and incidence angle. Repeated EROC/ENROL-based TS measurements on monospecific schools should result in accurate TS(L) equations for small pelagic fish species, near normal incidence.

Supplementary material

The following supplementary material is available at ICESJMS online:

295   Table 4. Results of on-axis calibration performed at 10, 30, 55 and 70 m depth.

Figure 11. Effect of depth on EROC echosounder calibration parameters.

Figure 12. Example of single echo detection on 1 ping, with respect to the acoustic samples uncompensated (a), compensated (b) Target Strengths and alongship (c) and athwartship (d) angles. Acoustic samples selected at each step are shown with different symbols. Acoustic samples finally retained are in light blue.

300 Figure 13. Target tracking example, displaying the target depth (a), athwartship and alongship positions (b), Target Strength (c) and speed (d). The target has entered the acoustic beam on top (positive alongship position in (b)), and has been tracked over 64 pings. Target Strength (TS) variations can be related to incidence angle changes (+/-5° with 8dB compensation). Target speed variations could be caused by a swimming behavior, with alternate active swimming and passive gliding.

310   References

Andersen, L. 2005. Status and plans for the ER60/EK60. ICES WGFAST Report, 2005/B:05: 20.

Balk, H., Lindem, T. 2003. Sonar5–Pro, post processing system.Operator manual.
http://folk.uio.no/hbalk/exchange_files/Manual_SonarX%20v601%20for
%20printing_28_03_2012.pdf

Barange, M. 1994. Acoustic identification, classification and structure of biological patchiness on
the edge of the Agulhas Bank and its relation to frontal features. S. Afr. J. Mar. Sci, 14: 333–
347.

Barange, M., Hampton, I., and Soule, M. 1996. Empirical determination of target strengths of three
loosely aggregated pelagic fish species. ICES J. Mar. Sci., 53: 225–232.

Doray, M., Badts, V., Massé, J., Duhamel, E., Huret, M., Doremus, G., and Petitgas, P. 2014.
Manual of fisheries survey protocols. PELGAS surveys (PELagiquesGAScogne). Manuel
des protocoles de campagne halieutique Ifremer, 30259.
http://archimer.ifremer.fr/doc/00191/30259/28714.pdf.

Doray, M., Josse, E., Gervain, P., Reynal, L., and Chantrel, J. 2006. Acoustic characterisation of
pelagic fish aggregations around moored fish aggregating devices in Martinique (Lesser
Antilles). Fish. Res., 82: 162–175.

Doray, M., Josse, E., Gervain, P., Reynal, L., and Chantrel, J. 2007. Joint use of echosounding,
fishing and video techniques to assess the structure of fish aggregations around moored Fish
Aggregating Devices in Martinique (Lesser Antilles). Aquatic Living Resources, 20: 357–
366.

Faessler, S. M. M., O'Donnell, C., and Jech, J. M. 2013. Boarfish (Capros aper) target strength
modelled from magnetic resonance imaging (MRI) scans of its swimbladder. ICES Journal
of Marine Science, 70: 1451–1459.

Foote, K. G. 1980. Importance of the swimbladder in acoustic scattering by fish: A comparison of
gadoid and mackerel target strengths. J. Acoust. Soc. Am, 67: 2084–2089.

Foote, K. G. 1987. Fish target strengths for use in echo integrator surveys. J. Acoust. Soc. Am, 82:
981–987.

Foote, K. G., Knudsen, H. P., Vestnes, G., MacLennan, D. N., and Simmonds, E. J. 1987.
Calibration of acoustic instruments for fish density estimation: a practical guide. ICES
Coop. Res. Rep., 144: 57.

Fréon, P., and Misund, O. A. 1999. Dynamics of pelagic fish distribution and behaviour: effects on
fisheries and stock assessment. Blackwell, Oxford.

Horne, J. K. 2000. Acoustic approaches to remote-species identification: a review. Fish.Oceanogr,
9: 356–371.

ICES 1999.Method for target strength measurements.*ICES Cooperative Research Report*, *235*, 59.

ICES. 2005. Description of the ICES HAC standard data exchange format, version 1.60. *ICES
Cooperative Research Report*, 278: 86.

ICES 2008. Report of the Working Group on Acoustic and Egg Surveys for Sardine and Anchovy in
ICES Areas VIII and IX (WGACEGG). ICES CM, 2008/LRC:17: 183.

Jech, J., and Horne, J. K. 2001.Effects of in situ target spatial distributions on acoustic density
estimates. ICES Journal of Marine Science, 58: 123–136.

Kubilius, R., and Ona, E. 2012.Target strength and tilt-angle distribution of the lesser sandeel
(*Ammodytesmarinus*). Ices Journal of Marine Science, 69: 1099–1107.

McClatchie, S., Alsop, J., and Coombs, R. F. 1996. A re-evaluation of relationships between fish
size, acoustic frequency, and target strength. ICES Journal of Marine Science, 53: 780–791

O'Driscoll, R. L., Oeffner, J., and Dunford, A. J. 2013. In situ target strength estimates of optically verified southern blue whiting (*Micromesistiusaustralis*). Ices Journal of Marine Science, 70: 431–439.

Ona, E. 2003. An expanded target-strength relationship for herring. ICES Journal of Marine Science, 60: 493–499.

Peltonen, H., and Balk, H. 2005. The acoustic target strength of herring (*Clupeaharengus* L.) in the northern Baltic Sea. ICES Journal of Marine Science, 62: 803–808.

Rose, G. 1992. A review of problems and new directions in the application of fisheries acoustics on the Canadian east coast. Fish. Res, 14: 105-128.

Ryan, T. E., Kloser, R. J., and Macaulay, G. J. 2009. Measurement and visual verification of fish target strength using an acoustic-optical system attached to a trawlnet. ICES Journal of Marine Science, 66: 1238–1244.

Sawada, K., Takahashi, H., Abe, K., Ichii, T., Watanabe, K., and Takao, Y. 2009. Target-strength, length, and tilt-angle measurements of Pacific saury (*Cololabissaira*) and Japanese anchovy (*Engraulisjaponicus*) using an acoustic-optical system. ICES Journal of Marine Science, 66: 1212–1218.

Simmonds, E. J., and MacLennan, D. N. 2005. Fisheries Acoustics. Theory and Practice. Blackwell publishing, Oxford, UK. 456 pp.

Soule, M., Barange, M., and Hampton, I. 1995. Evidence of bias in estimates of target strength obtained with a split-beam echo-sounder. ICES J. Mar. Sci, 52: 139–144.

Soule, M., Barange, M., Solli, H., & Hampton, I. (1997). Performance of a new phase algorithm for discriminating between single and overlapping echoes in a split-beam echosounder. *ICES Journal of Marine Science: 54*(5), 934-938.

Stanton, T. K. 1988. Sound scattering by cylinder of finite length. I. Fluid cylinders. Journal of the Acoustical Society of America, 83: 55–63.

Stanton, T. K. 1989. Sound scattering by cylinder of finite length. III. Deformed cylinders. Journal of the Acoustical Society of America, 86: 691–705.

Trenkel, V. M., Berger, L., Bourguignon, S., Doray, M., Fablet, R., Massé, J. & Villalobos, H. (2009). Overview of recent progress in fisheries acoustics made by Ifremer with examples from the Bay of Biscay. Aquatic Living Resources, 22(04), 433-445.

Wardle, C. S. 1975. Limit of fish swimming speed. Nature, 255: 725–727.

Zhao, X., Wang, Y., and Dai, F. 2008. Depth-dependent target strength of anchovy (*Engraulis japonicus*) measured in situ. ICES J. Mar. Sci., 65: 882–888.

Appendix 1: single echo detection and tracking method

Our Matlab implementation of the Soule et al (1997) algorithm is similar to those used in other acoustic data post processing systems (e.g. EK60, Andersen 2005, Echoview, www.echoview.com, Sonar5, Balk and Linderm 2003). Based on S_v, alongships and athwartships phase angles values stored in HAC files, Target Strength (TS) compensated (TS_{comp}) or uncompensated (TS_{uncomp}) for beam pattern are computed, as well as TS_{uncomp} values uncompensated for transmission losses (P_{like}), derived as: $P_{like}= TS_{uncomp}- 40logR-2.\alpha.R$, where α is the absorption coefficient and R the range to the transducer. The beam pattern compensation is computed using the Simrad's small angle approximation for a weighted transducer as: $TS = TS_{uncomp}+ 6.0206*(x^2+y^2-0.18*x^2.*y^2)$, with $x=2.(al-ofs_{al})/\Theta_{al}$ and $y=2.(at-ofs_{at})/\Theta_{at,}$ where al and at are the alongships and athwartships angles, ofs_{al} and ofs_{at} are the alongship and athwartship calibrated steering offsets, and Θ_{al} and Θ_{at} are the alongships and athwartships one-way 3-dB beamwidths.

The single targets detection method comprises the following steps, illustrated in Figure 12 in supplementary material:

1. Selecting initial single echoes candidates as: i) echoes whose P_{like} value is a local maximum ($P_{like-max}$), and ii) echoes whose TS values are higher than a user defined threshold.

2. Filtering based on echo length. The echo length is defined as the number of samples before and after $P_{like-max}$, for which P_{like} values are higher than $P_{like-max}$-6dB. The echo is retained if its length falls between user defined, minimum and a maximum normalized pulse length values.

3. Filtering based on maximum beam compensation values, computed as: TS_{comp}-TS_{uncomp}. Echoes with maximum beam compensations lesser than a user-defined threshold are retained.

4. Filtering based on phase angles, to filter out echoes that are not angularly coherent over a pulse duration, defined as five consecutive samples around $P_{like-max}$. Echoes whose alongships and athwartships phase angles standard deviations are lower than a used-defined threshold are retained.

5. Filtering based on distance to stronger neighbouring echo. A fine scale range is computed for each retained local maxima, as the average of the $P_{like-max}$ samples ranges, weighted by the P_{like} sample values over the echo length. An accurate transmission loss compensation is computed for each echo,

based on their fine scale range. Echoes are finally retained if their distance to the nearest echo displaying a stronger $P_{like-max}$ is higher than a user defined threshold.

The retained single echoes are then tracked, using the following method, illustrated in Figure 13 in supplementary material:

1. Single echoes positioning and track initialisation. The positions of all single targets are computed in a geographic coordinate system defined by an origin at the position where data acquisition started, an x-axis in the horizontal plane, with positive values to the North, a y-axis in the horizontal plane, with positive values to the East, and a z axis with positive values downwards. Each single echo is initially considered as a track.

2. Distance-based target tracking. The following target tracking procedure is iteratively applied on all pings, starting at ping number N=1. Assuming that the EROC follows the vessel track at the same speed, the distances between each single target in ping N+1 and all single echoes in ping N are computed, based on inter-ping times, target ranges and vessel speed. A single echo s_{N+1} in ping N+1 is assigned to the track comprising the single echo s_N in ping N if the distance between s_N and s_{N+1} is smaller than a user-defined maximum displacement between 2 consecutive pings, and if s_N is the closest single echo to s_{N+1}. If no single echo s_N satisfies these conditions, computations in step 2 are performed on single targets in pings N+1 and N-1, allowing for a 1 echo gap between 2 consecutive targets in the tracks. If ping N-1 does not exist, or if no single echo satisfying the conditions is found in ping N-1, s_{N+1} is associated to no single echo in previous pings.

3. Track length and wholeness filtering. Tracks with a number of single echoes and a relative number of gaps respectively higher and lesser than user-defined thresholds are actually retained.

Tables

365   **Table 1. Target Strength detection parameters**

Parameter	Movies3D	Simrad
Pulse length	0.128 ms	0.128 ms
Min. threshold	-60 dB	-60 dB
Min-Max echolength	[0.8 – 1.8]	[0.8 – 1.8]
Maximum Gain Compensation	5 dB	8 dB
Max. phase deviation	5	8
Min echo spacing	1	1

Table 2. Summary statistics of selected anchovy Target Strengths (TS) datasets. SD = standard deviation

| Dataset	1	2	3	4	Average (SD)
Date	05/31/15	05/31/15	06/01/15	06/01/15	
Start time	17:15:00	17:31:17	11:28:42	11:30:14	
End time	17:18:00	17:33:22	11:29:36	11:31:08	
Duration (s)	180	125	54	54	103 (61)
Ping rate (no. Ping.s-1)	20	20	17	17	18 (2)
EROC depth average (SD) (m)	49.8 (0.4)	51 (0.3)	55.4 (0.9)	56.1 (0.2)	51.7 (2.6)
EROC depth variation per track (SD) (m)	0.008 (0.007)	0.02 (0.01)	0.04 (0.03)	0.03 (0.01)	0.02 (0.01)
EROC roll average (SD) (°)	3.6 (1.5)	4.5 (1.6)	2.8 (1.4)	3.9 (0.9)	4.1 (1.4)
EROC pitch average (SD) (°)	1.1 (1.0)	0.2 (0.8)	6.3 (2.8)	5.1 (2.4)	3.2 (3)
No. of tracks Movies3D / Simrad	13 / 6	16 / 7	25 / 5	21 / 10	19 (5) / 7 (2)
Total No. of TS in tracks Movies3D / Simrad	186 / 75	267 / 143	458 / 110	364 / 167	319 (118) / 124 (40)
Movies3D / Simrad No. of TS in tracks average (SD)	14 (3) / 13 (2)	17 (6) / 20 (9)	18 (11) / 22 (16)	17 (5) / 17 (6)	17 (2) / 18 (4)
Movies3D / Simrad TS average (5;95% quantiles) (dB)	-43.7 (-46.3;-41.9) /-44.1(-46.7;-41.9)	-43.2(-45.3;-41.3) / -43.7(-47.4 ;-41)	-43.3(-46.8;-41.8) / -44(-47.7;-42)	-43.1(-45.9;-41.2) / -43.3(-46.3;-41.7)	-43.3(-46.3;-41.5) / -43.7(-47.2;-41.7)
Movies3D global target heading relative vessel heading during track average (SD) (°)	-4.7 (4.7)	-7.8 (7.6)	-2.8 (8.3)	-1.9 (7)	-4.3 (2.6)
Movies3D global target pitch angle during track average (SD) (°)	-0.2 (0.7)	0 (0.6)	-1 (0.7)	-0.8 (0.5)	-0.5 (0.1)

370

375

Table 3. Average and standard deviation (SD) of the morphological parameters derived from X-ray tomographic (CT) imaging of 5 *Engraulis encrasicolus* specimen.

Parameter	Value
Fish length average (SD) (cm)	10.5 (0.5)
Swimbladder length average (SD) (cm)	3 (0.2)
Swimbladder to fish length ratio average (SD) (%)	28.3 (1.2)
Swimbladder surface average (SD) (cm^2)	2.9 (0.4)
Swimbladder volume average (SD) (cm^3)	0.3 (0.06)
Swimbladder equivalent cylinder aspect ratio average (SD) (unitless)	10.1 (0.5)
Swimbladder tilt angle average (SD) (°)	4.2(0.9)
Swimbladder equivalent cylinder curvature angle average (SD) (°)	10° (3.6°)

Figures

385
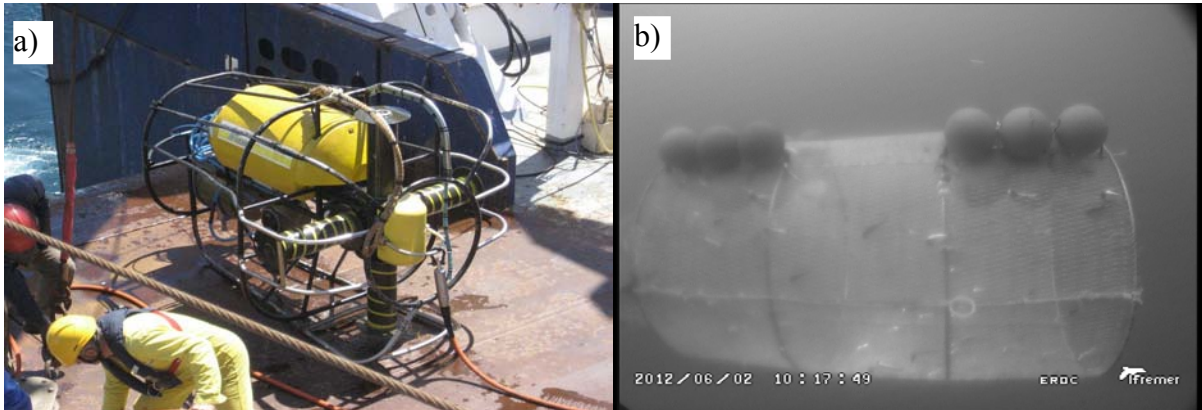
390 Figure 1: a) Remotely Operated Towed Vehicle EROC, b) Underwater picture of the open codend ENROL taken by the EROC camera.
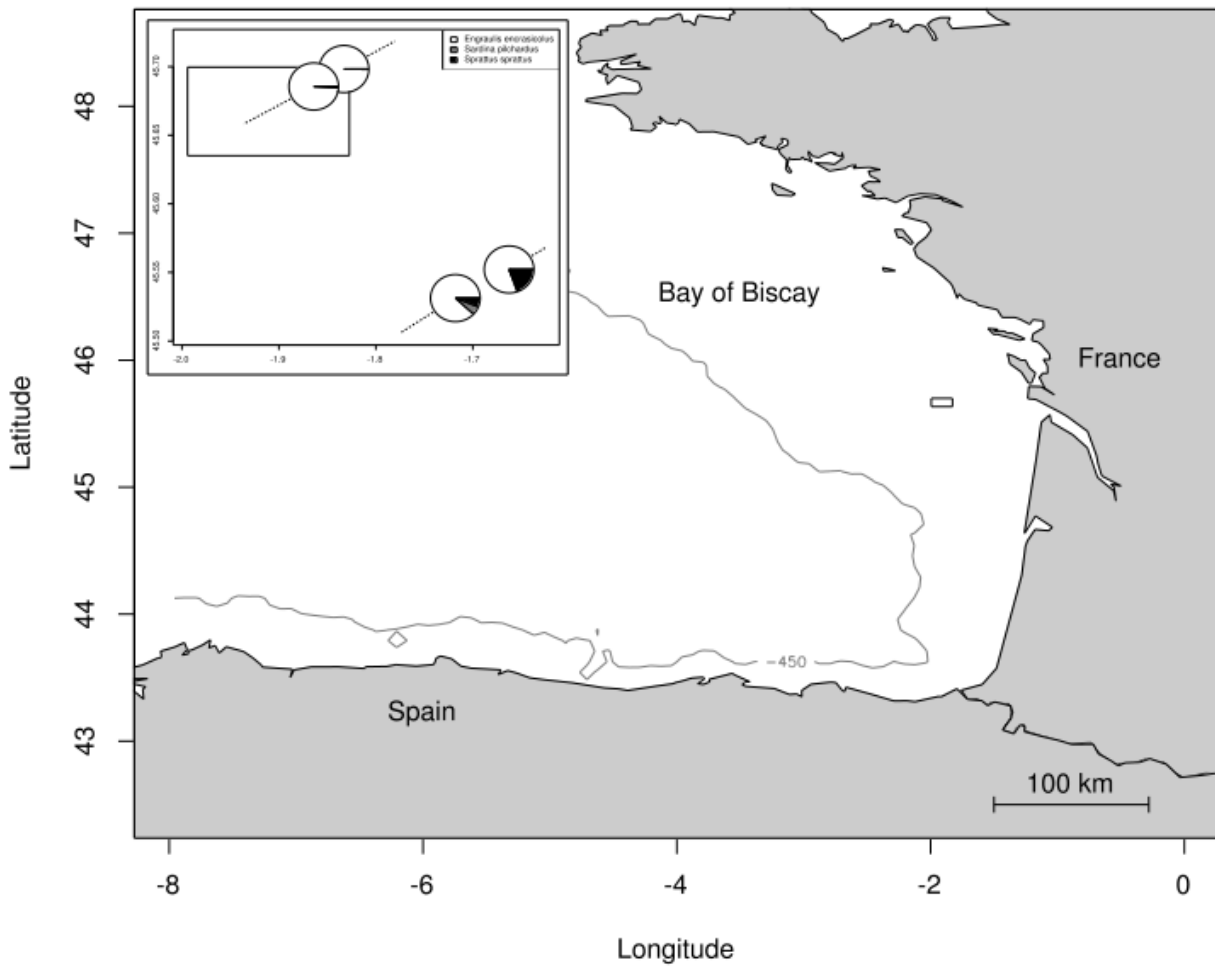
Figure 2. Bay of Biscay map showing the 450m isobath (continental shelf limits, grey line) and the area where anchovy Target Strengths (TS) were recorded (black rectangle). The upper-left panel is a zoom on the study area showing the TS recording area (black rectangle), the paths of the 4 identification trawl hauls (dotted lines), and pie charts presenting the trawl catch relative composition (*Engraulis engrasicolus* in white, *Sardina pilchardus* in grey and *Sprattus sprattus* in black).
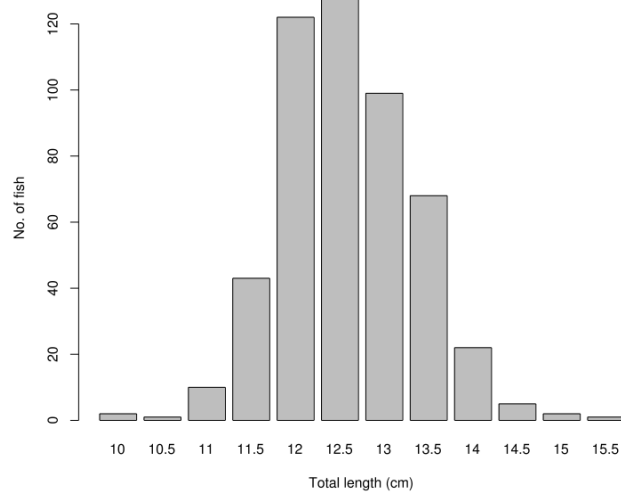
Figure 3: Histogram of the length distribution of *Engraulis encrasicolus* caught in the study area (N=4 trawl hauls, mean anchovy proportion in the catch: 88%).
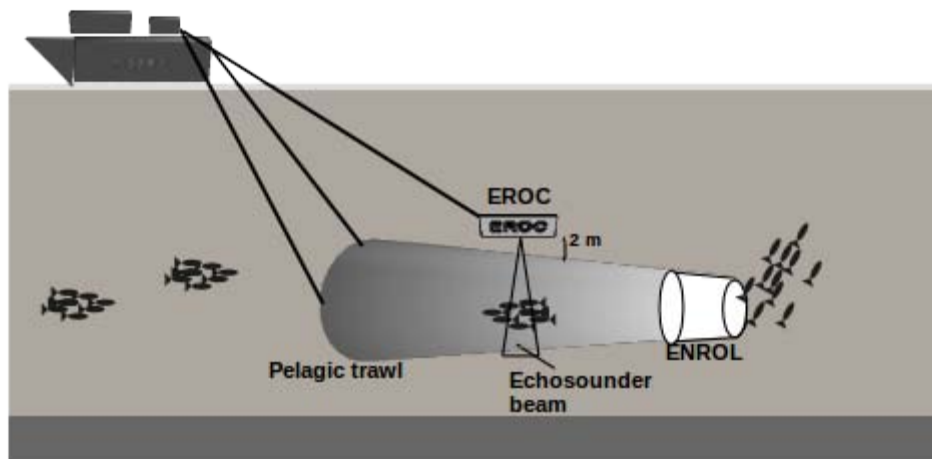
405   Figure 4. Scheme of the EROC-ENROL Target Strength recording configuration.
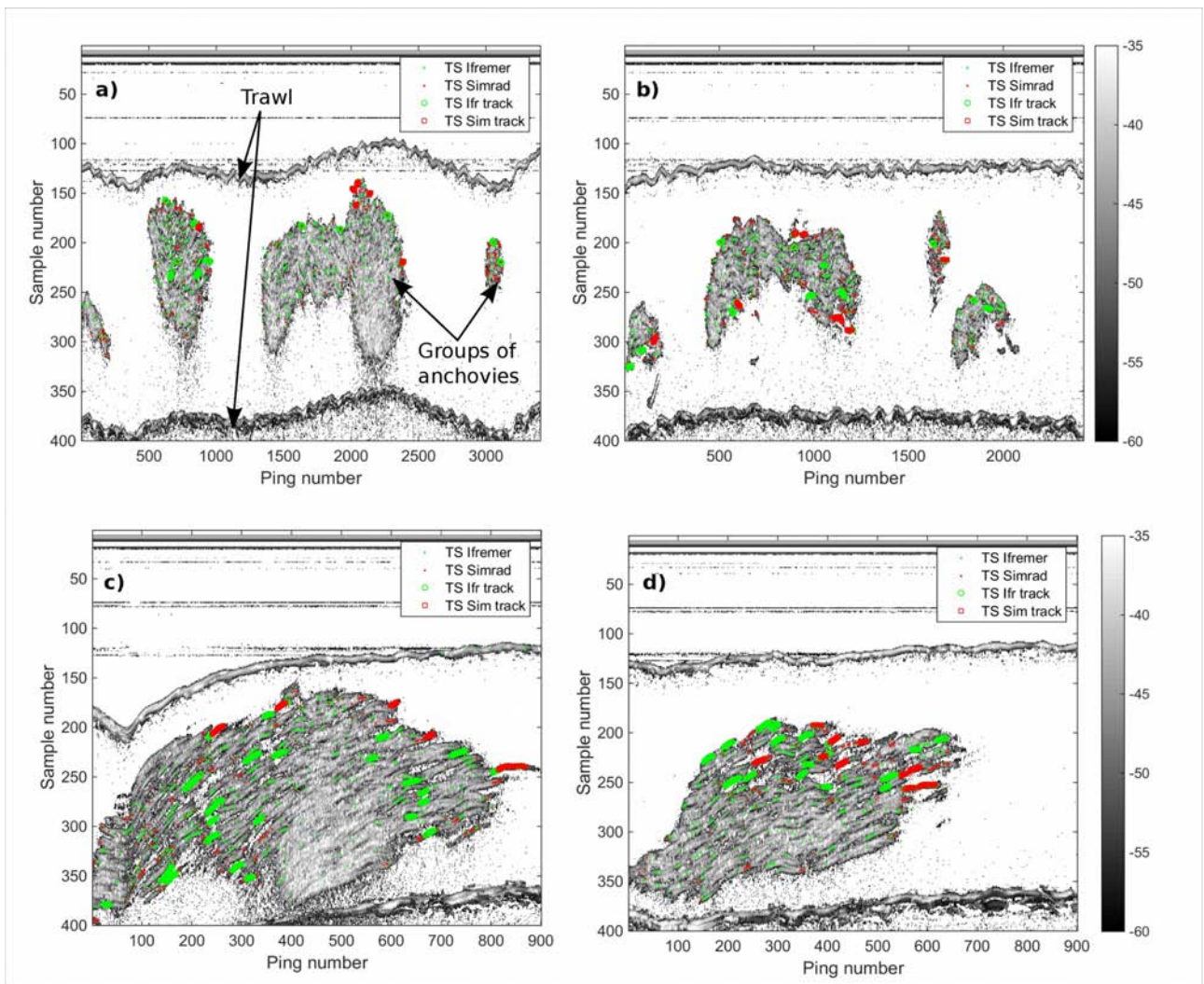
Figure 5: Echograms showing groups of anchovies swimming in a pelagic trawl. Echograms recorded on: a) 05-31-2015 between 17:15:00 and 17:18:00, b) 05-31-2015 between 17:31:17 and 17:33:22, c) 06-01-2015 between 11:28:42 and 11:29:36, d) 06-01-2015 between 11:30:14 and 11:31:08. Acoustic densities, expressed as volume backscattering coefficients (S_V in dB), are in grey scale. Small red square dots: single targets detected using Simrad's algorithm, large red empty squares: tracked single targets detected using Simrad's algorithm, small green dots: single targets detected using Movies3D implementation of Soule et al. (1997)'s algorithm, large green empty circles: tracked single targets detected using Movies3D implementation of Soule et al. (1997)'s algorithm.
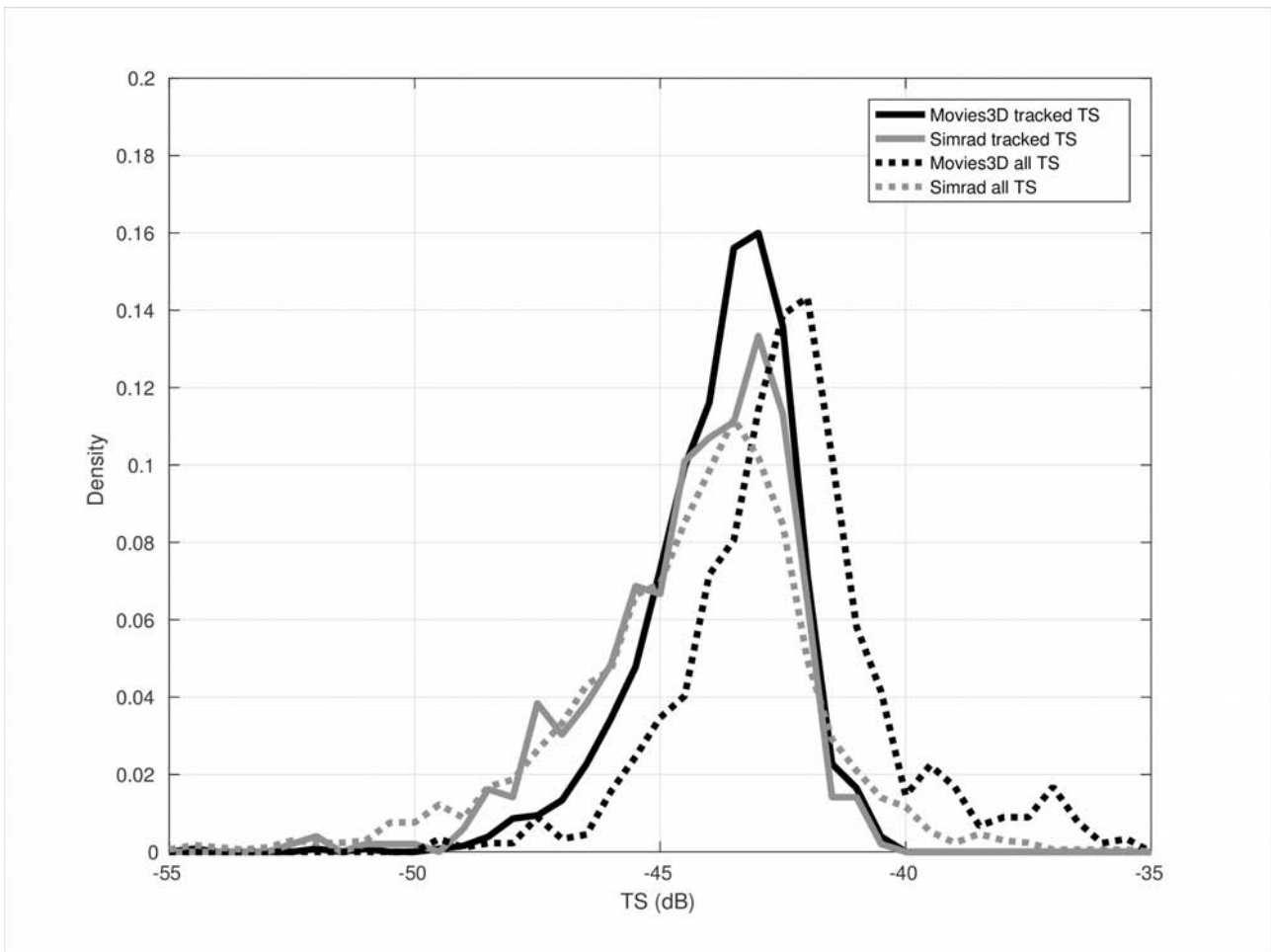
Figure 6. Distributions of *Engraulis encrasicolus* Target Strength (TS, in dB) distributions recorded with the EROC-ENROL system. Black solid line: TS distribution after target tracking of single echoes detected using the Movies3D implementation of Soule et al. (1997) algorithm. Grey solid line: TS distribution after target tracking of single echoes detected using Simrad's algorithm. Black dotted line: TS distribution of single echoes detected using the Movies3D implementation of Soule et al. (1997) algorithm. Grey dotted line: TS distribution of single echoes detected using Simrad's algorithm.

420
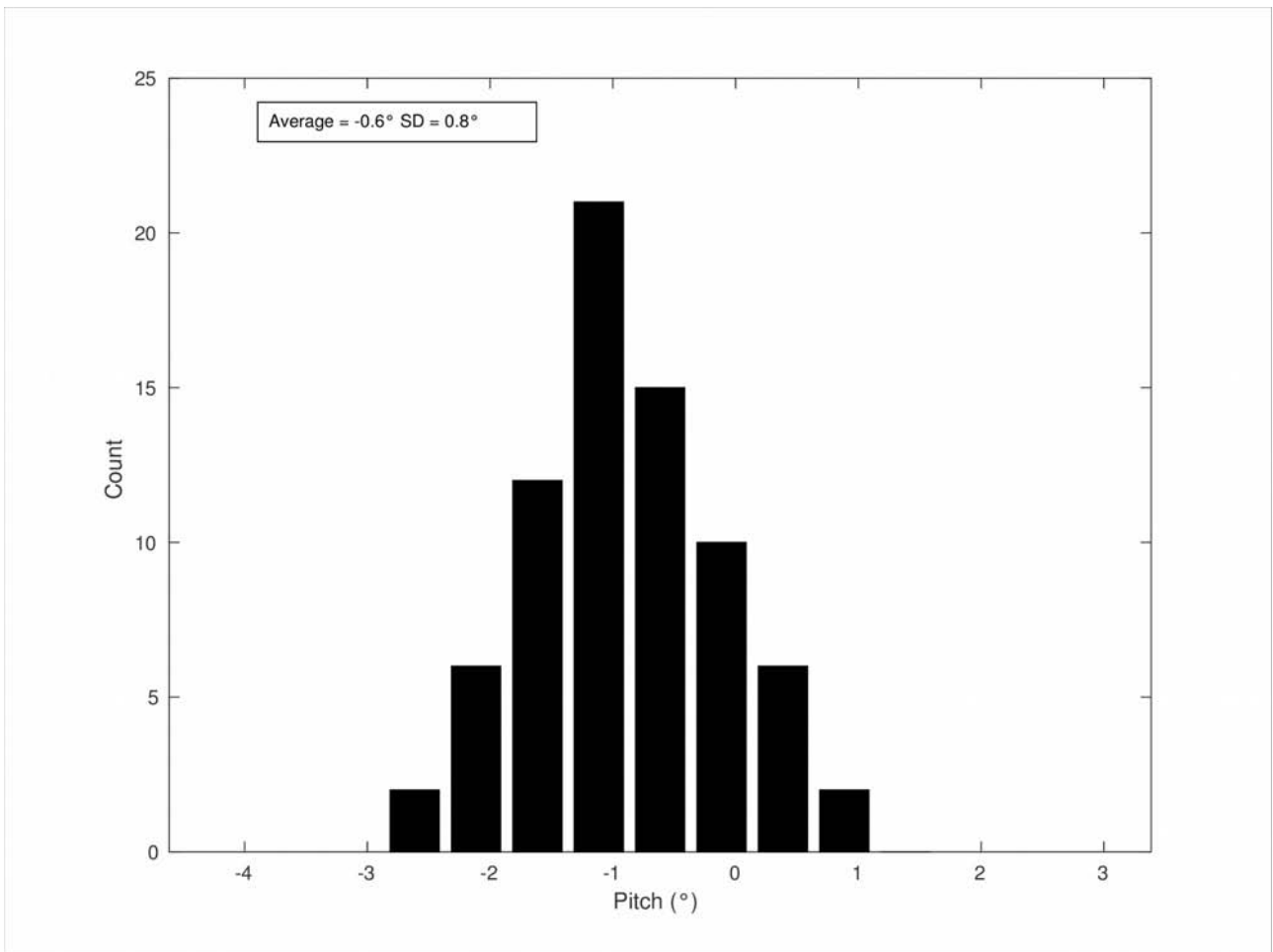
Figure 7. Distribution of fish targets global pitch angles during tracks in all 4 datasets (mean = -0.6°, standard deviation (SD) = 0.8°).
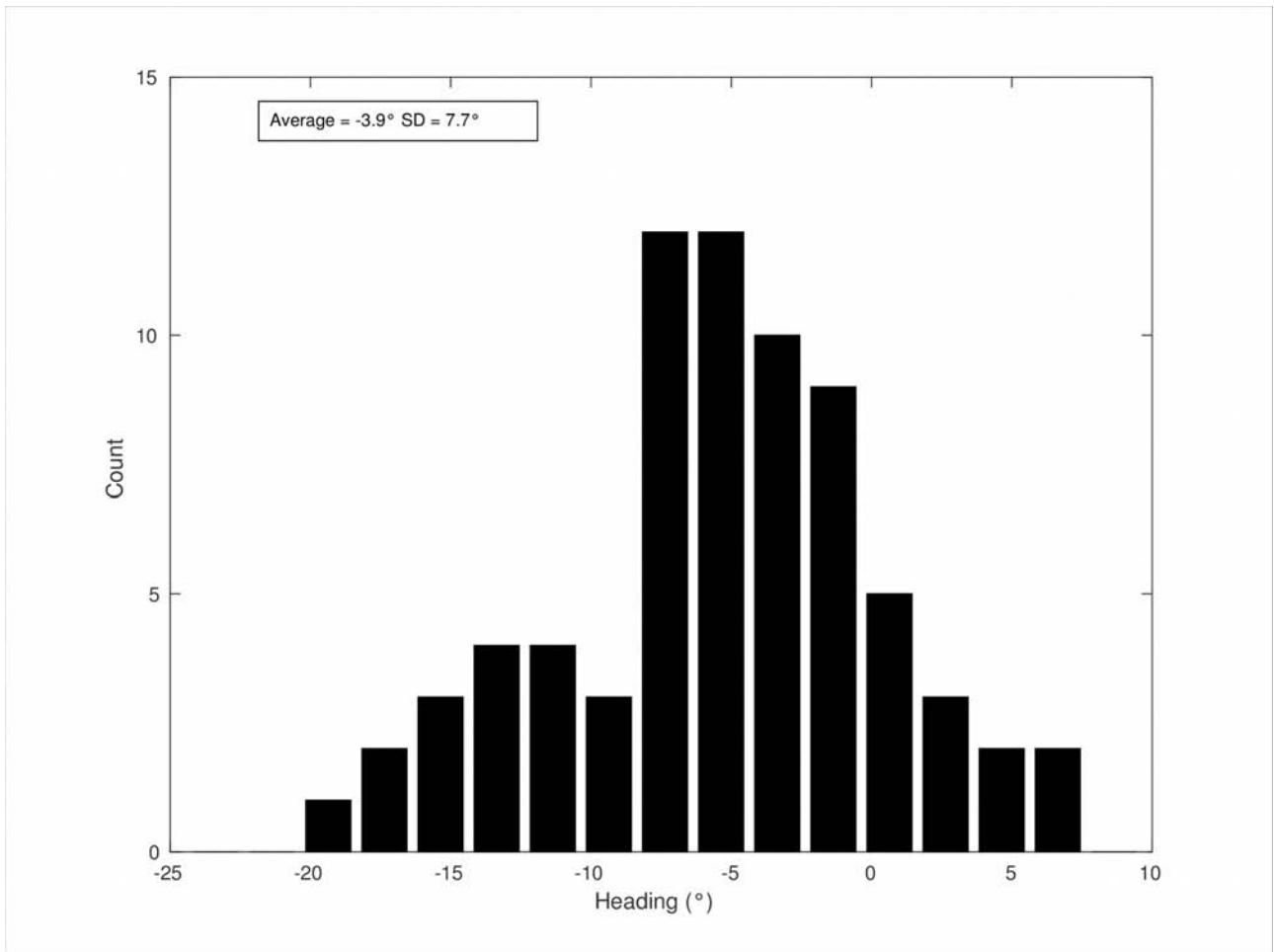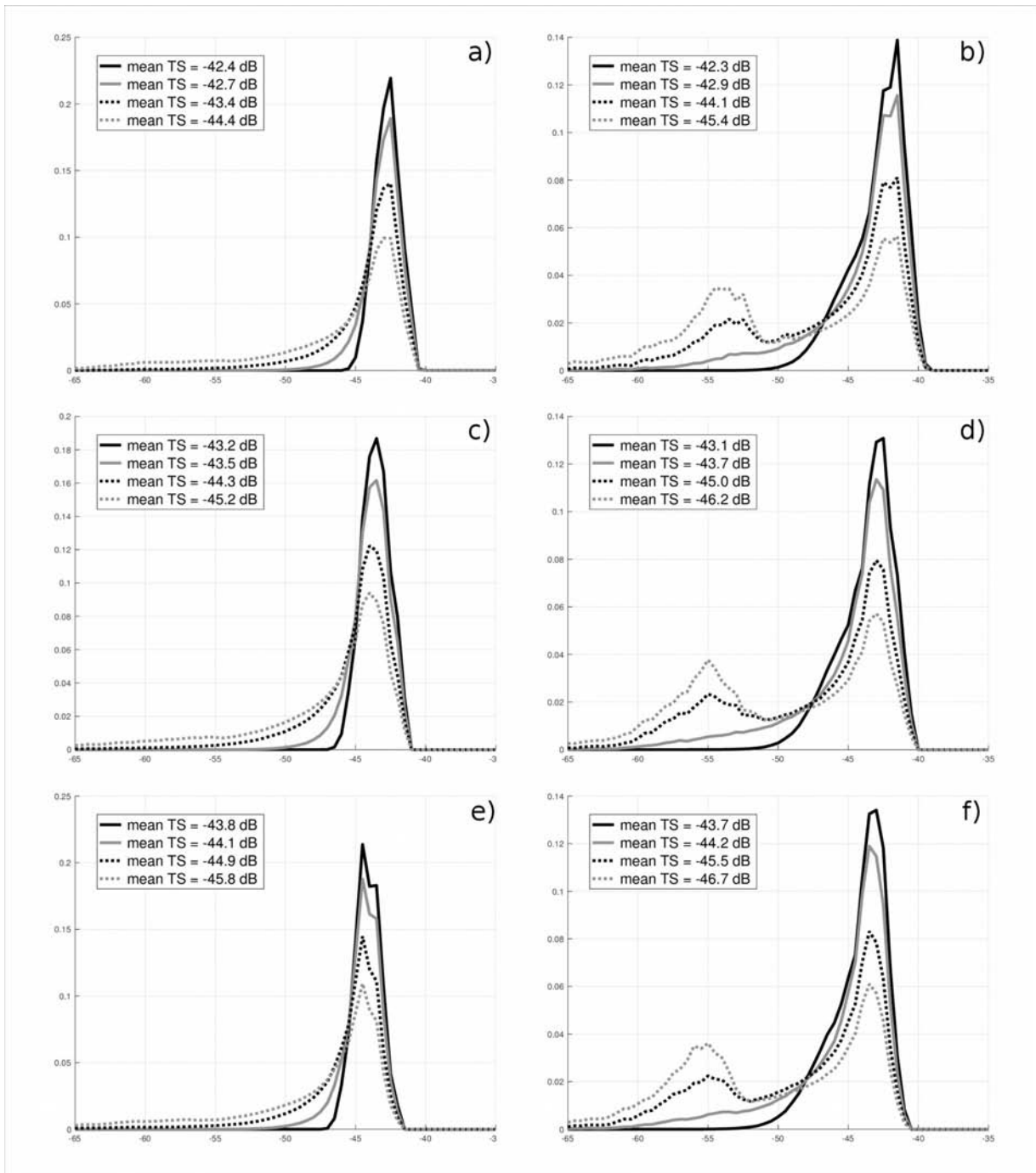
Figure 8. Distribution of fish headings in the horizontal plane during tracks, relatively to the vessel heading (0° = vessel heading, fish headings average = -3.9°, standard deviation (SD) = 7.7°).

430

435

Figure 10. *Engraulis encrasicolus* Target Strength (TS, in dB) distributions modelled at 38kHz (Figures a, c, e) and 70kHz (Figures b, d, f) for 3 swimbladder aspect ratios (Fig. a&b: 10, Fig. c&d: 15, and Fig. e&f: 20) and four fish tilt angle distributions: black solid lines: N(-0.5°,1), grey solid lines: N(-0.5°,5), black dotted lines: N(-0.5°,10), grey dotted lines N(-0.5°,15).

Supplementary material

Table 4. Results of on-axis calibration performed at 10, 30, 55 and 70 m depth.

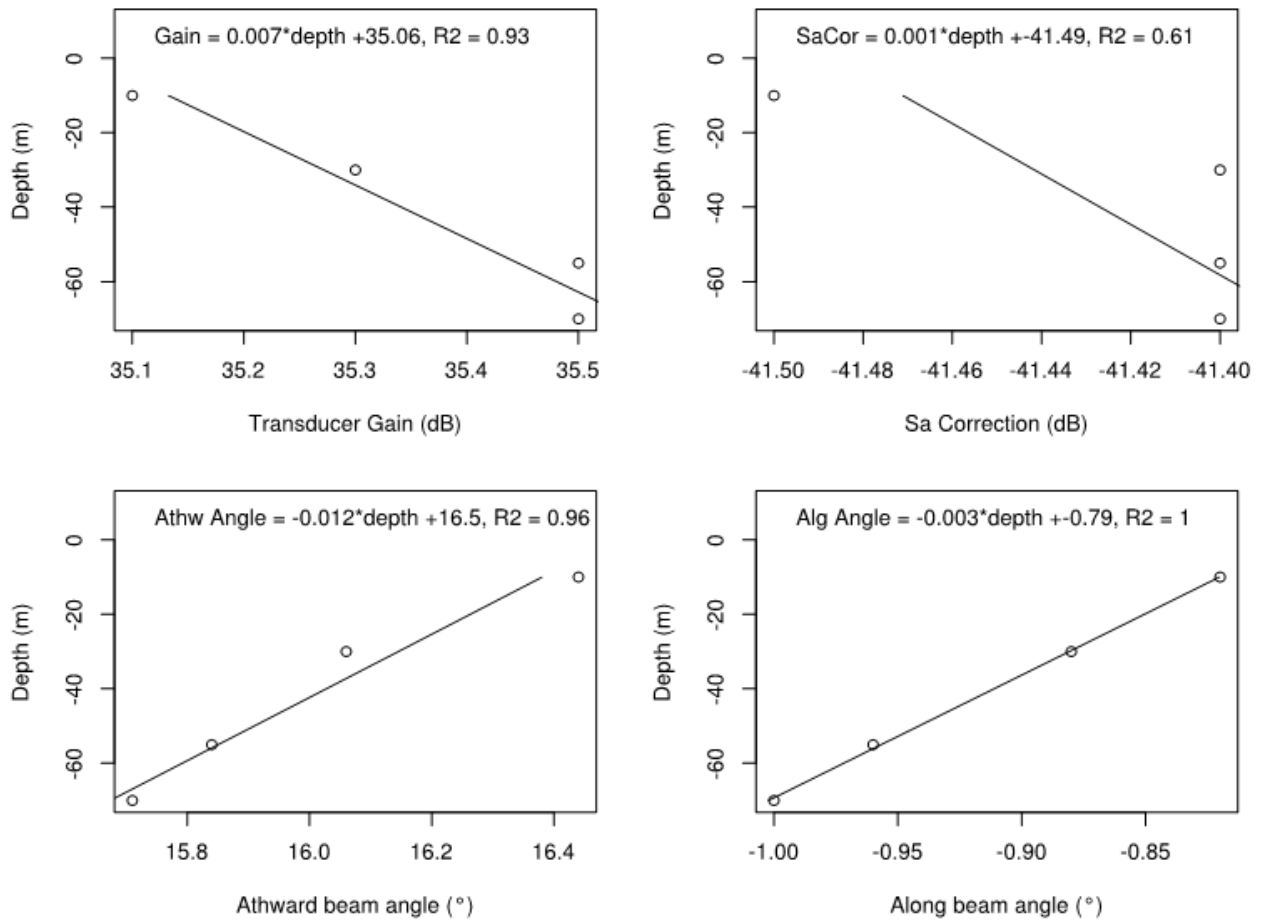| Depth (m)	10	30	55	70	Average	SD
Temperature (°C)	13,7	11,2	11,3	11,2	11,9	1,21
Salinity (PSU)	35,1	35,3	35,5	35,5	35,4	0,19
Sphere TS (dB)	-41,5	-41,4	-41,4	-41,4		
Transducer Gain (dB)	16,44	16,06	15,84	15,71	15,82	0,28
Sa Correction (dB)	-0,82	-0,88	-0,96	-1	-0,90	0,07
Athw. Beam Angle (°)	6,89	6,88	6,92	6,63	6,83	0,11
Along. Beam Angle (°)	6,74	6,69	6,7	6,59	6,69	0,07
Athw. Offset Angle (°)	0	-0,03	-0,09	-0,05	-0,03	0,03
Along. Offset Angle (°)	-0,06	-0,04	-0,06	-0,07	-0,06	0,02
Data deviation from beam model (RMS in dB)	0,19	0,19	0,24	0,23	0,20	0,02
Data deviation from polynomial model (RMS in dB)	0,12	0,14	0,21	0,19	0,15	0,02

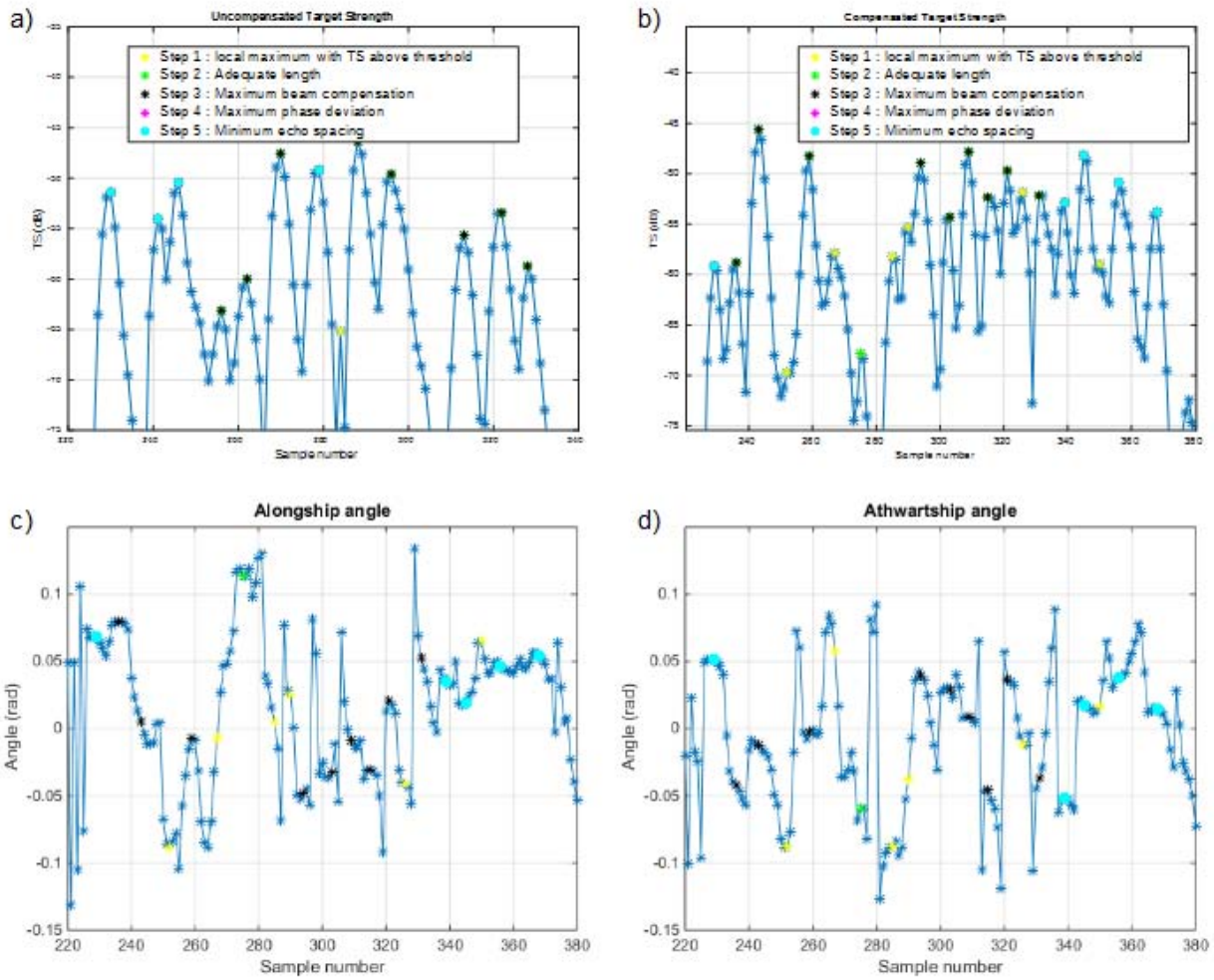Figure 11. Effect of depth on EROC echosounder calibration parameters

Figure 12. Example of single echo detection on 1 ping, with respect to the acoustic samples uncompensated (a), compensated (b) Target Strengths and alongship (c) and athwartship (d) angles. Acoustic samples selected at each step are shown with different symbols. Acoustic samples finally retained are in light blue.
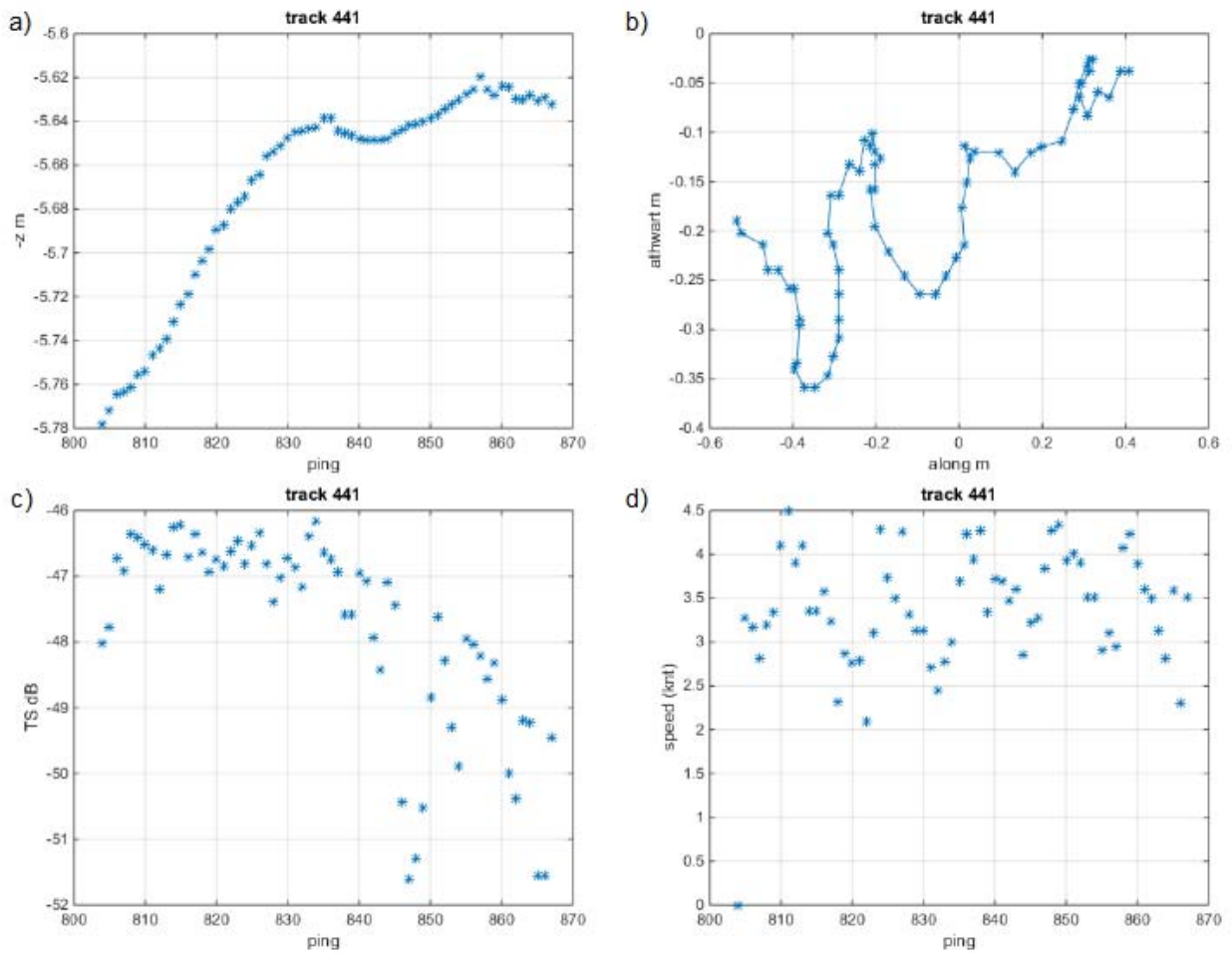
450

Figure 13. Target tracking example, displaying the target depth (a), athwartship and alongship positions (b), Target Strength (c) and speed (d). The target has entered the acoustic beam on top (positive alongship position in (b)), and has been tracked over 64 pings. Target Strength (TS) variations can be related to ensonifying angle changes (+/-5° with 8dB compensation). Target speed variations could be caused by a swimming behavior, with alternate active swimming and passive gliding.